

En-face choroidal vascularity map of the macula in healthy eyes

Sumit Randhir Singh^{1,2}, Mohammed Abdul Rasheed¹,
Nishad Parveen³, Abhilash Goud¹, Samatha Ankireddy⁴,
Niroj Kumar Sahoo¹, Kiran Kumar Vupparaboina⁵,
Soumya Jana³ and Jay Chhablani¹

European Journal of Ophthalmology
1–8

© The Author(s) 2019

Article reuse guidelines:

sagepub.com/journals-permissions

DOI: 10.1177/1120672119883593

journals.sagepub.com/home/ejo



Abstract

Purpose: To report the en-face choroidal vascularity index in healthy eyes.

Methods: Thirty eyes of 30 healthy individuals were studied. Multiple high-density cross-sectional swept source optical coherence tomography scans were obtained to create a volume scan. The choroid was segmented for the whole volume scan and choroidal inner boundaries were flattened. Subsequently, multiple en-face scans separated by 25 μ m were obtained and binarized. Choroidal vascularity index was calculated at level of choriocapillaris, medium, and large choroidal vessels.

Results: The mean age of the study cohort was 35.6 ± 8.8 years. The overall mean en-face choroidal vascularity index was $54.25 \pm 0.55\%$. There was a statistically significant difference of choroidal vascularity index in choriocapillaris ($53.16 \pm 0.43\%$), medium choroidal vessel ($51.38 \pm 0.27\%$), and large choroidal vessel ($55.69 \pm 0.87\%$) ($p < 0.01$). Choroidal vascularity index analysis in three subgroups based on subfoveal choroidal thickness (low: $< 300 \mu$ m, medium: $300\text{--}400 \mu$ m, high: $> 400 \mu$ m) showed a statistically significant difference ($p = 0.001$). Choroidal vascularity index showed a significant correlation with subfoveal choroidal thickness ($r = 0.441$; $p = 0.015$), whereas there was no significant correlation of age ($p = 0.21$), refraction ($p = 0.20$), and gender ($p = 0.67$) with en-face choroidal vascularity index.

Conclusion: En-face choroidal vascularity index shows a significant variation at the level of choriocapillaris, medium choroidal vessel, and large choroidal vessel in normal eyes. Choroidal vascularity index reaches a nadir at the level of medium choroidal vessel and reaches the maximum value at large choroidal vessel near choroidoscleral interface. En-face choroidal vascularity index shows a significant physiological variation and appears to increase with increase in subfoveal choroidal thickness.

Keywords

En-face optical coherence tomography, choroidal vascularity index, choriocapillaris, choroidal thickness

Date received: 2 August 2019; accepted: 28 September 2019

Introduction

The choroid is comprised primarily of blood vessels and, from outward to inward, includes large (Haller's layer; LCV), medium (Sattler's layer; MCV) choroidal vessels, and layer of the choriocapillaris (CC).¹ This vascular layer provides the majority of blood supply to the eye. The role of vascular choroid has been shown in a variety of chorioretinal disorders including age-related macular degeneration (AMD), pachychoroid spectrum-related disorders, and high myopia.^{2,3} With advances in imaging techniques, there is an increasing interest in the choroid and its vascularity. The introduction of enhanced depth imaging optical

¹Smt. Kanuri Santhamma Centre for Vitreo Retinal Diseases, L V Prasad Eye Institute, Hyderabad, India

²Retina and Uveitis Department, L V Prasad Eye Institute, Visakhapatnam, India

³Department of Electrical Engineering, Indian Institute of Technology Hyderabad, Hyderabad, India

⁴School of Medicine, University of Missouri–Kansas City, Kansas City, MI, USA

⁵Srujana Innovation Center, L V Prasad Eye Institute, Hyderabad, India

Corresponding author:

Jay Chhablani, Smt. Kanuri Santhamma Centre for Vitreo Retinal Diseases, L V Prasad Eye Institute, Banjara Hills, Hyderabad 500034, Telangana, India.

Email: jay.chhablani@gmail.com

coherence tomography (EDI-OCT) and swept source optical coherence tomography (SS-OCT), which uses a longer wavelength (1050 nm), has facilitated the detailed evaluation of the choroidal morphology and vascularity.⁴⁻⁶ Multiple studies have studied different choroidal parameters such as choroidal thickness, volume, vessel layer thickness, vascularity index (CVI) using axial B scans at subfoveal and extrafoveal locations reaching up to mid equator in normal and/or diseased eyes.⁶⁻¹⁸

En-face OCT is one of the recent additions which provides a coronal view of the retina and choroid.^{19,20} Often termed as C scan, these differ from conventional B scans and can be obtained from volume data generated using closed spaced scans in newer, high-definition OCT machines.^{19,20} En-face scans provide in vivo spatial localization of choroidal vessels or any chorioretinal pathology with a detailed analysis of morphological changes in a single view.

En-face imaging has been used to study the choroidal vascular pattern and calculate the vascular area along with vascular diameter.²¹⁻²⁴ Sohrab et al. have reported the choroidal vascular changes in normal, eyes with early AMD and reticular pseudodrusen using en-face images at three levels (CC, MCV, and LCV). However, these scans have remained confined to few specified planes and were unable to provide minute details of the vascularity of choroid throughout the entire thickness of choroid.^{21,23} Previous histopathological studies have provided information about choroidal vasculature especially the choriocapillaris in normal and diseased eyes.²⁵ Previous reports have shown significant loss and reduction of CC diameter in eyes with early, intermediate, advanced AMD with geographic atrophy and neovascular AMD. However, the sample size was small in various subgroups and outer choroidal layers were not evaluated.²⁵

Choroidal vascularity index (CVI), a ratio of vascular luminal area versus total choroidal area, has been studied extensively using axial B scan data in normal and multiple chorioretinal disorders.^{7-11,26-29} This in vivo, noninvasive choroidal parameter can be applied on en-face scans and can provide a truer representation of the choroidal vasculature as seen in real life. Here, we report the CVI changes of macular area in healthy individuals using en-face OCT images generated through volume maps and provide details about the changes in choroidal vascularity through entire choroidal thickness at every 25 μm .

Materials and methods

This was an observational, cross-sectional study involving 30 eyes of 30 healthy volunteers conducted at a tertiary setup in India from December 2017 to May 2018. Prior institutional review board approval was obtained and study conformed to the tenets of the Declaration of Helsinki.

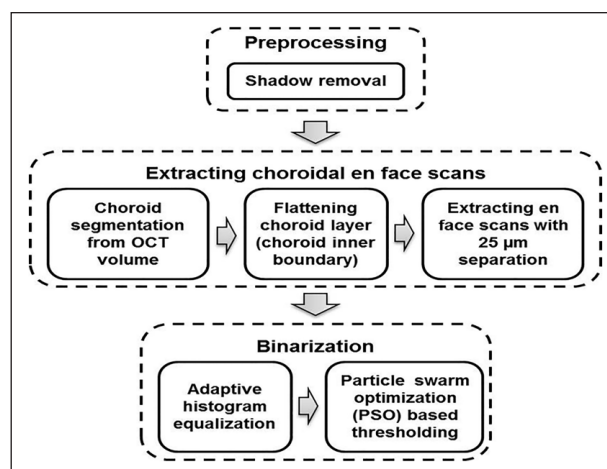


Figure 1. A brief schematic depicting the steps involved in the estimation of en-face CVI of healthy eyes.

The enrolled volunteers were explained about the procedure and study-related risks, and a written informed consent was taken from the study participants. A thorough history and comprehensive ocular examination was done to rule out any significant ocular and systemic pathology. Ocular examination included best-corrected visual acuity (BCVA) in Snellen visual acuity chart, anterior segment, and fundus examination using slit lamp and indirect ophthalmoscopy, respectively, intraocular pressure (IOP) and refraction. Exclusion criteria included BCVA <20/20, refraction $\geq \pm 3$ D, eyes with significant media opacities, macular pathologies, any prior intraocular surgeries or laser or history of any systemic diseases like diabetes mellitus or hypertension.

SS-OCT imaging

For each eye, a volume scan containing multiple high-density cross-sectional OCT scans was obtained using DRI OCT Triton, SS-OCT (Topcon, Tokyo, Japan) with a scanning speed of 100,000 A-scans/s. A total of 256 unaveraged cross-sectional scans per acquisition were taken. These data were exported from the Topcon device as image stacks (8-bit gray scale).

The schematic of the proposed methodology for obtaining en-face CVI measurement is depicted in Figure 1. The algorithm mainly involves (1) extracting choroidal en-face scans and (2) binarization of en-face scans.

Extracting choroidal en-face scans

We first segmented the choroid from the OCT volume and then extracted en-face scans separated by 25 μm for CVI analysis. In particular, each B scan of the volume was analyzed to segment choroid based on previously validated algorithm where retinal pigment epithelium

(RPE)–Bruch’s complex and choroid–scleral interface (CSI) were identified using structural similarity (SSIM) index, Hessian analysis, and tensor voting.³⁰ Subsequently, segmented choroid sections were stacked to obtain the choroid volume and multiple en-face sections separated by 25 μm were generated.

En-face CVI estimation

In particular, the method employs adaptive histogram equalization and a window-based particle swarm optimization (PSO). Adaptive histogram equalization with a window size of 8×8 was employed (using built-in MATLAB function) to increase the contrast between the blood vessels and the stroma. Subsequently, blood vessels were segmented using PSO-based thresholding.

PSO technique has shown its superiority over conventional thresholding algorithms including fuzzy C-means and Otsu techniques for multidimensional biomedical images, especially retinal blood vessel segmentation.^{31,32}

PSO is an efficient optimization technique, inspired by bird flocking, which iteratively improves a candidate solution based on the defined fitness function. It tries to move particles (candidate solutions) around in the search space iteratively based on particles position and velocity, where each particle’s movement is influenced by its local best and global best values among the overall population of the swarm.

Noting the non-uniformity in the pixel intensities of vascular regions as well as stromal regions across the image, we performed block-based PSO. For each block, we obtained the threshold by iteratively updating particle velocities and positions defined by

$$v_i^{(t+1)} = w^{(t)}v_i^{(t)} + C_1r_1 \left[p_i^{(t)} - x_i^{(t)} \right] + C_2r_2 \left[g_i^{(t)} - x_i^{(t)} \right]$$

and

$$x_i^{(t+1)} = x_i^{(t)} + v_i^{(t+1)}$$

where $v_i^{(t)}$ and $x_i^{(t)}$ are the velocities of the i th particle in the t th iteration. Furthermore, $p_i^{(t)}$ is the particle’s best position and $g_i^{(t)}$ is the swarm’s best position. $w^{(t)}$ is the inertia weight, C_1, C_2 (empirically fixed at 0.6) are the acceleration constants and r_1, r_2 are the random number stacking values between (0, 1). For implementation, we considered particle population size of 15, number of iterations as 250 and inertia weight was chosen empirically as 1. The segmentation performance of the proposed methodology was validated using observer grading inspired from similar problem reported earlier. In particular, two observers graded the percentage of choroid vasculature correctly segmented in binarized en-face images in comparison with choroid vasculature in the original en-face image. The grading was done twice by both the observers blinded to

each other as well as their own gradings. We found a concordance rate of 0.97–0.99 for various levels of en-face images.

CVI was calculated separately at all the en-face images separated every 25 μm . We sought to understand whether the average of CVI measurement at three defined points based on the prior anatomical information is reflective of the overall mean CVI involving multiple equidistant en-face planes. The layer of small choroidal vessel including choriocapillaris was defined as a dense network of small vessels just beneath the Bruch’s membrane. Three points of measurements were identified manually in each eye based on the above description at the level of the choriocapillaris (at 10 μm below RPE–Bruch’s membrane), junction of MCV and LCV (junction of one-third and two-thirds of subfoveal choroidal thickness; SFCT) and just inner to CSI adjacent to the LCVs. Representative image showing original, shadow compensated and binarized en-face scans is shown in Figure 2.

In addition, total study population of 30 eyes was subdivided into three subgroups (<300 μm , 300–400 μm , and >400 μm) based on SFCT and CVI was compared in the three subgroups. The coefficient of variation (CV) of CVI was calculated in each vascular layer of choroid to identify the variation of the CVI in the study eyes.

Statistical analysis was done using SPSS v22 (SPSS Inc., Chicago, IL, USA). The choroidal parameters were recorded as the mean \pm standard deviation (SD). Normality of the data was determined and analysis of variance (ANOVA) was used to study the variation of CVI in different choroidal layers and in subgroups with different SFCT. Correlation between CVI and age, gender, and refraction was determined using linear regression and significant values were subjected to multivariate regression analysis. Only $p \leq 0.05$ was considered statistically significant.

Results

Thirty eyes of 30 healthy individuals with a mean (\pm SD) age of 35.6 ± 8.8 years (range: 23–47 years) were studied. Only one eye (right eye) per subject was used for analysis. The study population comprised 17 males and 13 females. The average spherical equivalent was -0.10 ± 0.48 D (range: -1 to $+1$ D). The mean SFCT of the study eyes was $352.75 \pm 85.06 \mu\text{m}$.

In our cohort, mean choroidal volume was $5.59 \pm 1.13 \text{ mm}^3$ (range: 3.50 – 7.88 mm^3). The total bright (stromal) and dark (luminal) region volume were 2.50 ± 0.51 (range: 1.59 – 3.52 mm^3) and 3.05 ± 0.63 (range: 1.86 – 4.31 mm^3), respectively. This variation in volume arises due to variation in choroidal thickness of the study eyes.

The overall en-face CVI in the study population ($n=30$) including the mean of CVI at each of the 25- μm en-face planes was $54.25 \pm 0.55\%$. The mean en-face CVI at CC,

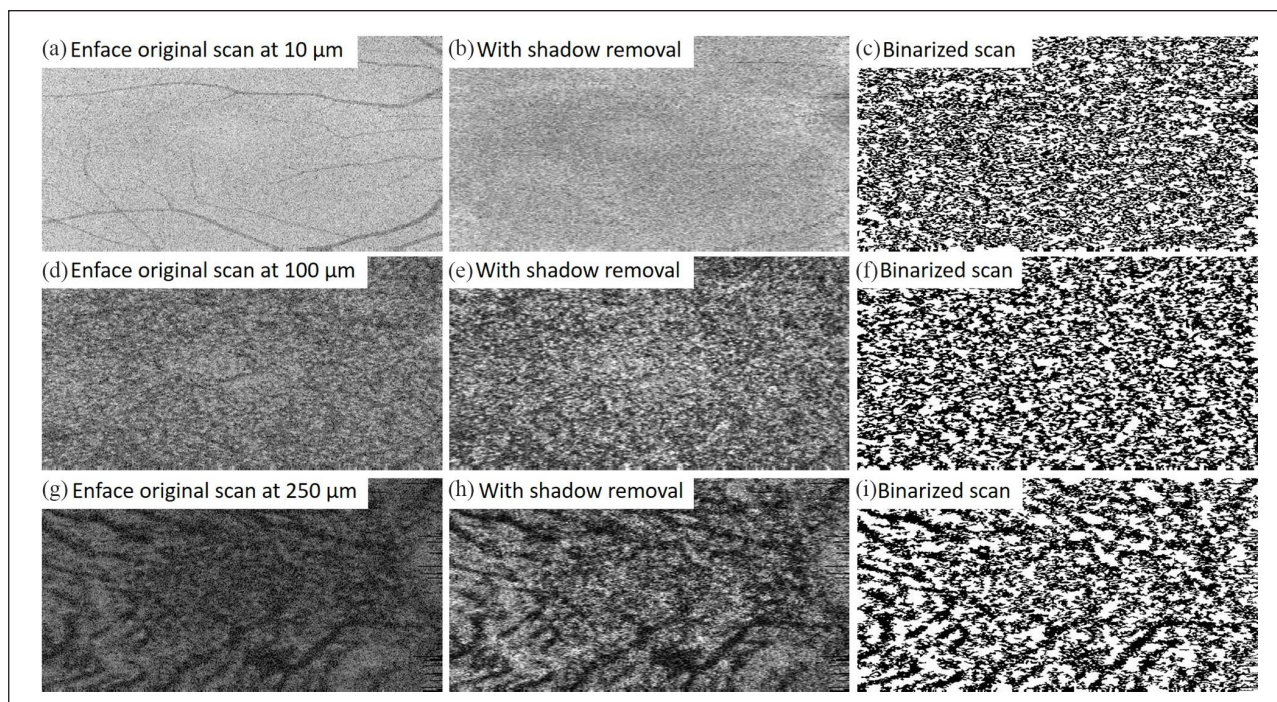


Figure 2. (a, d, g) En-face (OCT) images at different choroidal depths. The shadow-compensated en-face scans show better contrast enhancement with removal of shadows from overlying layers and are depicted in (b), (e), (h). (c, f, i) Post binarization, the extracted en-face scans show vascular lumen as dark and choroidal stroma as white areas, respectively.

Table 1. Choroidal vascularity index (CVI) in eyes with different subfoveal choroidal thickness (SFCT; low: <300 μm, medium: 300–400 μm, high: >400 μm).

SFCT (μm)	Overall	Choroidal vascularity index (CVI; %)		
		Choriocapillaris	Medium choroidal vessel	Large choroidal vessel
<300 (n=10)	53.80 ± 0.64	53.14 ± 0.31	51.23 ± 0.20	55.17 ± 1.10
300-400 (n=14)	54.56 ± 0.32	53.13 ± 0.48	51.39 ± 0.25	56.14 ± 0.56
>400 (n=6)	54.26 ± 0.31	53.27 ± 0.56	51.59 ± 0.32	55.52 ± 0.50
Total (n=30)	54.25 ± 0.55	53.16 ± 0.43	51.38 ± 0.27	55.69 ± 0.87
p value*	0.001	0.80	0.03	0.01

*p values were calculated using analysis of variance (ANOVA) comparing CVI in the three subgroups based on SFCT. Pairwise comparisons using Tukey post hoc test were done if p value was statistically significant ($p \leq 0.05$). The significant differences in the pairwise comparison are highlighted in bold.

MCV, and LCV levels was $53.16 \pm 0.43\%$, $51.38 \pm 0.27\%$, and $55.69 \pm 0.87\%$, respectively (Table 1). The difference of CVI among the three vascular layers of choroid using one-way ANOVA was statistically significant ($p < 0.01$). The Tukey post hoc analysis revealed a significant difference between all three subgroups (CC vs MCV, $p < 0.01$; CC vs LCV, $p < 0.01$; MCV vs LCV, $p < 0.01$). There was a 3.35% reduction of mean en-face CVI from CC to MCV where CVI was least. Toward the outer choroid, mean en-face CVI increased to a maximum value near CSI (an increase in 4.76% as compared to en-face CVI at the level of CC).

The study cohort was divided into three subgroups based on SFCT (low: <300 μm, medium: 300–400 μm,

high: >400 μm). The mean en-face CVI recorded in these subgroups was $53.80 \pm 0.64\%$, $54.56 \pm 0.32\%$, and $54.26 \pm 0.31\%$ respectively, ($p = 0.001$). Post hoc analysis revealed significant difference of CVI between eyes with low and medium SFCT ($p = 0.001$). Pairwise comparison of mean en-face CVI between low versus high SFCT ($p = 0.14$) and medium versus high SFCT ($p = 0.35$) revealed no significant differences. The comparison of en-face CVI of CC ($p = 0.80$), MCV ($p = 0.03$), and LCV ($p = 0.01$) in the three SFCT subgroups is detailed in Table 1. CVI of MCV varied in eyes with low and high SFCT ($p = 0.025$). Similarly, there was a significant difference of CVI of LCV between low and medium SFCT ($p = 0.01$).

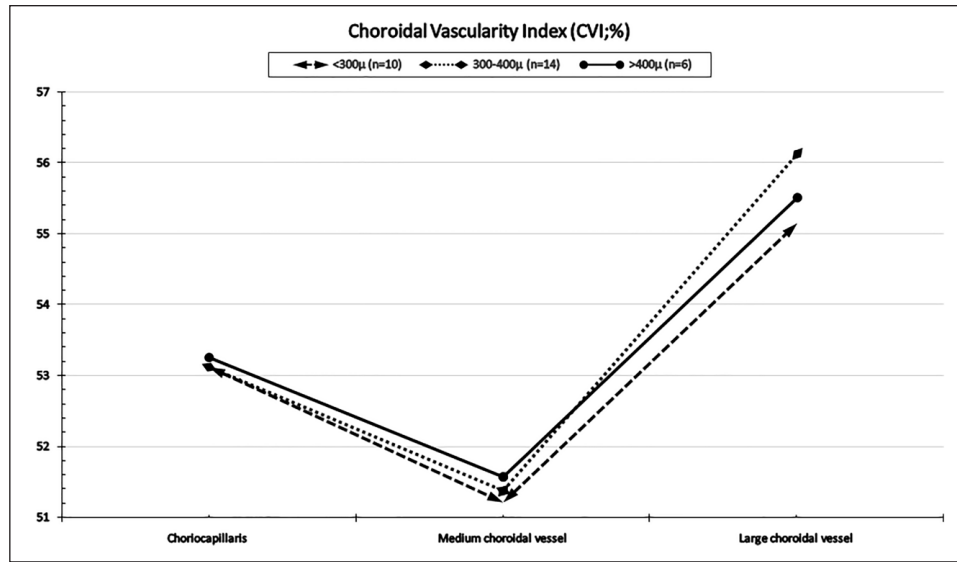


Figure 3. A graph showing the variation of choroidal vascularity index (CVI in eyes with different subfoveal choroidal thickness (SFCT: <300 µm, 300–400 µm, and >400 µm). CVIs at the level of choriocapillaris, medium, and large choroidal vessels in each subgroup are also shown.

Figure 3 shows a graph showing the comparison of CVI at CC, MCV, and LCV in eyes with different SFCT.

Overall mean en-face CVI of total volume scan was compared to the mean CVI at three pre-determined points at different levels of choroidal thickness as described earlier. There was significant difference between the overall mean CVI compared to mean CVI of three defined points ($54.25 \pm 0.55\%$ vs 55.17 ± 0.83 ; $p=0.001$). Pairwise comparison at each of these three points with the mean CVI at three levels (CC, MCV, and LCV) revealed a statistically significant difference at the level of LCV ($p=0.001$), whereas MCV ($p=0.18$) and CC ($p=0.99$) were not significantly different.

The CV (SD/mean) was derived for the CVI readings in the full volume scans. Maximum and minimum CV was seen in LCV (0.016) and MCV (0.005), respectively. The overall mean CV was 0.01 which was suggestive of the minimal variability of CVI in the study cohort. The mean coefficient of variation of SFCT was 0.24.

CVI showed a significant correlation with SFCT ($r=0.441$; $p=0.015$). Linear regression comparing overall en-face CVI with age ($p=0.21$), refraction ($p=0.20$), and gender ($p=0.67$) showed no significant correlation. Multiple regression analysis after adjusting for other variables failed to reveal any significant correlation of SFCT with en-face CVI ($p=0.19$).

Discussion

We studied the variation of CVI in normal eyes using en-face OCT scans and noted that mean CVI tends to reduce (a reduction of 3.35%) as the distance from RPE–Bruch’s

membrane increases to reach a nadir at the approximate junction of inner one-third and outer two-thirds (i.e. junction of MCV and LCV) and then increases toward CSI (an increase of 4.76%) as compared to CVI at the level of CC. Mean CVI at the level of CC just beneath the Bruch’s membrane was 53.16% and reached a minimum of 51.38% at the level of MCV. This further increased to reach a point of highest CVI at the level of LCV (55.69%) near CSI. This is suggestive of the increase in stromal component of the choroid in the middle portion of the choroid.

Sohrab et al., in their study using spectral-domain optical coherence tomography (SD-OCT), reported an average vascular density in CC (76.5%), Sattler’s layer (83.6%), and Haller’s layer (87.2%) with the highest density in Haller’s layer in normal eyes ($n=14$).²¹ The authors studied en-face scans (6 mm×6 mm and 0.5 mm×0.5 mm) at only three sections and the choroidal luminal and stromal differentiation was done on the basis of specific red, green, and blue (RGB) intensity. The cut-off pixel intensity was kept at 65 for each R, G, and B. Thicker choroid was found to be associated with higher vascular density in their study eyes.²¹ In another study in normal eyes, Ueda-Arakawa et al.²³ using SS-OCT showed that vascular density at the level of mid-point of RPE and CSI was $45.3 \pm 6.4\%$. The discrepancy between measurements is probably due to the different binarization techniques and this difference has been shown in previous reports as well.^{33,34} Moreover, mean age of control group in the study by Ueda-Arakawa et al.²³ (77.1 years), and Sohrab et al.²¹ (61 years) was much higher compared to mean age of our cohort (35.6 years). Both SD-OCT and SS-OCT were used to estimate CVI in the previous studies. Differences in CVI

arising due to different instrumentation are less likely as our group has previously shown moderate to good reliability of CVI measurements using both machines.³⁵

There was a significant difference in CVI in three vascular layers (CC, MCV, and LCV) which can be explained by the location and caliber of the blood vessels. The LCVs in the outer choroid have the highest CVI. This plays a role especially in the eyes with higher CT where the overall volume of LCV is much higher (as approximately 70% of CT is contributed by LCV) even though the CVI (being a ratio) is only marginally higher at the level of LCV. Whether the reduction in CVI at the level of MCV-LCV junction gets exaggerated with resultant compression by LCV leading to the development of pachychoroid spectrum disorders remains unanswered at present.

There were differences in CVI between the layers of the choroid based on SFCT as well. There was significant difference of CVI in MCV in the eyes with low and high SFCT. Similarly, CVI of LCV also was statistically different between eyes with low and medium SFCT. The disproportionate increase in the stromal component in these eyes with higher SFCT would explain this observation. The presence of reduced choroidal vascular density in innermost choroidal layers in eyes with reduced choroid thickness has been shown in previous studies also.²¹ However, the vascularity of outer choroidal layers was shown to be consistent unlike our study where CVI of CC, MCV, and LCV were noted to increase minimally with increase in SFCT.^{3,21}

The LCVs were found to have the highest CV (0.016) suggestive of the maximal variability in the luminal area. The CVI had a significant direct correlation of SFCT ($r=0.441$; $p=0.015$). This suggests that SFCT and CVI may have a moderate association with complex interplay of other factors such as age, gender, refraction, and axial length. However, CV of SFCT was 0.24 implying that SFCT is dependent on other factors and therefore CVI appears to be a more consistent parameter.

We noted a significant variation in CVI between three manually identified en-face planes when compared to the overall mean CVI ($p=0.0001$). However, the results were not surprising. The densely packed en-face OCT scans follow a continuum of small, medium, and large choroidal blood vessels with a gradual change of CVI at each level as expected in normal eyes. On the contrary, points at specified depths (CC, junction of one-third to two-thirds of SFCT and CSI) are abrupt measurement points and thus carry a steep gradient in CVI and may carry significant variation compared to the former approach. The reported CVI in previous studies may not have represented an accurate picture of choroidal vascularity.^{21,23}

The CVI was not found to vary significantly with respect to age, refraction, and SFCT (multivariate analysis). The reasons for this observation could be the limited age and refraction variability among the small study

sample. The luminal and total choroidal area may show certain variations in the healthy eyes. However, CVI being a ratio gets less affected and therefore shows lesser variation as compared to SFCT.

The study, however, has certain limitations. The normative data were available only at a single time point due to the cross-sectional nature of the study. There were a limited number of study participants, and considering the normal study subjects, these data cannot be extrapolated to different pathological conditions. The sample size was too small to accurately evaluate the relationship between CVI and age, refraction, and gender. The effect of diurnal variation on choroidal parameters, especially choroidal thickness, was not considered as the timing of OCT measurements was not available for all the study eyes. Although the repeatability of choroidal volume was not part of this study, estimation of choroidal volume among the initial few subjects produced consistent results on repeated measurements.

The demarcation between MCV and LCV was based on certain assumptions, and the true divide based on histopathology was not known. The calculation of CVI is based on the assumption of binarizing the choroid into bright and dark areas. Although en-face SS-OCT provides a superior view compared to cross-sectional OCT, however, it still not a true representative of histopathological section of choroid which has multiple components rather than a simple binary classification represented above.¹

It is expected that change in thresholding will lead to a variation in binarization. We therefore performed preprocessing (adaptive histogram equalization) to increase contrast between stromal and luminal regions. In other words, preprocessing attempted to clearly demarcate stromal and luminal histograms to facilitate optimal threshold measurements. Moreover, we used PSO-based segmentation techniques. The parameters of PSO including inertia weight, acceleration constants, particle population size, and number of iterations were optimized empirically and were consistent across all the images. Literature search reveals only one previous attempt made at segmenting choroid vessels using en-face OCT scans.³⁶ This method was based on level-set approach which was an iterative region-growing method. However, the accuracy of segmentation was not quantified and subjective evaluation of results suggests that there are spurious detections present in stromal regions. Perhaps, for the same reason, they restricted their work to only measure large vessel diameter interactively.³⁶ In addition to the aforementioned work, there have been attempts made at choroid layer binarization in OCT B scans. However, those methods were not fully automated and the threshold selection is subjective.³⁷ In comparison, our algorithm was fully automated and provided CVI values with shadow compensation.

In conclusion, we report another unique approach to assess choroidal vascularity by analysis of en-face CVI in

healthy eyes. En-face CVI was found to reach a nadir at the level of MCVs and then surges to reach the maximum value at choroidoscleral border. Future studies related to evaluating CVI changes in various disease conditions and a longitudinal follow-up can provide more detailed information about the sequential changes in CVI and insight into the pathogenesis.

Author contributions

S.R.S., M.A.R., K.K.V., J.C. were involved in the designing of the study. M.A.R., A.G., N.K.S., S.R.S. were involved in the collection of data. S.R.S., M.A.R., A.G., N.K.S., N.P., S.A., S.J., J.C. were responsible for interpretation and analysis of the data. S.R.S., M.A.R., S.A., K.K.V. were involved in manuscript writing. S.R.S., M.A.R., N.P., S.A., A.G., N.K.S., K.K.V., S.J., and J.C. reviewed the article. All the authors conducted the study and equally contributed in the preparation, review, and approval of the manuscript.

Data availability

All data were available upon request. In case of any further information, Dr Jay Chhablani can be contacted at jay.chhablani@gmail.com.

Declaration of conflicting interests

The author(s) declared no potential conflicts of interest with respect to the research, authorship, and/or publication of this article.

Funding

The author(s) received no financial support for the research, authorship, and/or publication of this article.

References

- Nickla DL and Wallman J. The multifunctional choroid. *Prog Retin Eye Res* 2010; 29: 144–168.
- Chhablani J, Wong IY and Kozak I. Choroidal imaging: a review. *Saudi J Ophthalmol* 2014; 28: 123–128.
- Sohrab MA and Fawzi AA. Review of en-face choroidal imaging using spectral-domain optical coherence tomography. *Med Hypothesis Discov Innov Ophthalmol* 2013; 2(3): 69–73.
- Zweifel SA, Engelbert M, Laud K, et al. Outer retinal tubulation: a novel optical coherence tomography finding. *Arch Ophthalmol* 2009; 127: 1596–1602.
- Choma M, Sarunic M, Yang C, et al. Sensitivity advantage of swept source and Fourier domain optical coherence tomography. *Opt Express* 2003; 11(18): 2183–2189.
- Hirata M, Tsujikawa A, Matsumoto A, et al. Macular choroidal thickness and volume in normal subjects measured by swept-source optical coherence tomography. *Invest Ophthalmol Vis Sci* 2011; 52(8): 4971–4978.
- Agarwal A, Agrawal R, Khandelwal N, et al. Choroidal structural changes in tubercular multifocal serpiginoid choroiditis. *Ocul Immunol Inflamm* 2017; 26: 838–844.
- Agrawal R, Li LKH, Nakhate V, et al. Choroidal vascularity index in Vogt-Koyanagi-Harada disease: an EDI-OCT derived tool for monitoring disease progression. *Transl Vis Sci Technol* 2016; 5(4): 7.
- Agrawal R, Salman M, Tan K-A, et al. Choroidal vascularity index (CVI)-a novel optical coherence tomography parameter for monitoring patients with panuveitis. *PLoS ONE* 2016; 11(1): e0146344.
- Agrawal R, Chhablani J, Tan K-A, et al. Choroidal vascularity index in central serous chorioretinopathy. *Retina* 2016; 36: 1646–1651.
- Tan R, Agrawal R, Taduru S, et al. Choroidal vascularity index in retinitis pigmentosa: an OCT study. *Ophthalmic Surg Lasers Imaging Retina* 2018; 49(3): 191–197.
- Singh SR, Invernizzi A, Rasheed MA, et al. Wide-field choroidal vascularity in healthy eyes. *Am J Ophthalmol* 2018; 193: 100–105.
- Jirattanasopa P, Ooto S, Tsujikawa A, et al. Assessment of macular choroidal thickness by optical coherence tomography and angiographic changes in central serous chorioretinopathy. *Ophthalmology* 2012; 119(8): 1666–1678.
- Sudhalkar A, Chhablani JK, Venkata A, et al. Choroidal thickness in diabetic patients of Indian ethnicity. *Indian J Ophthalmol* 2015; 63(12): 912–916.
- Chhablani J, Kozak I, Jonnadula GB, et al. Choroidal thickness in macular telangiectasia type 2. *Retina* 2014; 34: 1819–1823.
- Chhablani J, Rao PS, Venkata A, et al. Choroidal thickness profile in healthy Indian subjects. *Indian J Ophthalmol* 2014; 62: 1060–1063.
- Bartesselli G, Chhablani J, El-Emam S, et al. Choroidal volume variations with age, axial length, and sex in healthy subjects: a three-dimensional analysis. *Ophthalmology* 2012; 119(12): 2572–2578.
- Branchini LA, Adhi M, Regatieri CV, et al. Analysis of choroidal morphologic features and vasculature in healthy eyes using spectral-domain optical coherence tomography. *Ophthalmology* 2013; 120(9): 1901–1908.
- Flores-Moreno I, Arias-Barquet L, Rubio-Caso MJ, et al. En face swept-source optical coherence tomography in neovascular age-related macular degeneration. *Br J Ophthalmol* 2015; 99(9): 1260–1267.
- Pilotto E, Guidolin F, Convento E, et al. En face optical coherence tomography to detect and measure geographic atrophy. *Invest Ophthalmol Vis Sci* 2015; 56(13): 8120–8124.
- Sohrab M, Wu K and Fawzi AA. A pilot study of morphometric analysis of choroidal vasculature in vivo, using en face optical coherence tomography. *PLoS ONE* 2012; 7(11): e48631.
- Lehmann M, Wolff B, Vasseur V, et al. Retinal and choroidal changes observed with ‘en face’ enhanced-depth imaging OCT in central serous chorioretinopathy. *Br J Ophthalmol* 2013; 97(9): 1181–1186.
- Ueda-Arakawa N, Ooto S, Ellabban AA, et al. Macular choroidal thickness and volume of eyes with reticular pseudodrusen using swept-source optical coherence tomography. *Am J Ophthalmol* 2014; 157(5): 994–1004.
- Lau T, Wong IY, Iu L, et al. En-face optical coherence tomography in the diagnosis and management of age-related macular degeneration and polypoidal choroidal vasculopathy. *Indian J Ophthalmol* 2015; 63(5): 378–383.

25. Seddon JM, McLeod DS, Bhutto IA, et al. Histopathological insights into choroidal vascular loss in clinically documented cases of age-related macular degeneration. *JAMA Ophthalmol* 2016; 134(11): 1272–1280.
26. Ratra D, Tan R, Jaishankar D, et al. Choroidal structural changes and vascularity index in Stargardt disease on swept source optical coherence tomography. *Retina (Philadelphia, Pa.)* 2017; 38: 2395–2400.
27. Wei X, Ting DSW, Ng WY, et al. Choroidal vascularity index: a novel optical coherence tomography based parameter in patients with exudative age-related macular degeneration. *Retina* 2017; 37(6): 1120–1125.
28. Tan KA, Laude A, Yip V, et al. Choroidal vascularity index—a novel optical coherence tomography parameter for disease monitoring in diabetes mellitus. *Acta Ophthalmol* 2016; 94(7): e612–e616.
29. Giannaccare G, Pellegrini M, Sebastiani S, et al. Choroidal vascularity index quantification in geographic atrophy using binarization of enhanced-depth imaging optical coherence tomographic scans. *Retina*. Epub ahead of print 22 January 2019. DOI: 10.1097/IAE.0000000000002459.
30. Vupparaboina KK, Nizampatnam S, Chhablani J, et al. Automated estimation of choroidal thickness distribution and volume based on OCT images of posterior visual section. *Comput Med Imaging Graph* 2015; 46(Pt. 3): 315–327.
31. Hassan G, Hassanien AE, El-Bendary N, et al. Blood vessel segmentation approach for extracting the vasculature on retinal fundus images using particle swarm optimization. In: *2015 2011th international computer engineering conference (ICENCO)*, Cairo, 29–30 December 2015.
32. Lahmiri S and Boukadoum M. An evaluation of particle swarm optimization techniques in segmentation of biomedical images. In: *GECCO Comp'14 proceedings of the companion publication of the 2014 annual conference on genetic and evolutionary computation*, Vancouver, BC, Canada, 12–16 July 2014, pp. 1313–1320. New York: ACM.
33. Wei X, Sonoda S, Mishra C, et al. Comparison of choroidal vascularity markers on optical coherence tomography using two-image binarization techniques. *Invest Ophthalmol Vis Sci* 2018; 59(3): 1206–1211.
34. Vupparaboina KK, Dansingani KK, Goud A, et al. Quantitative shadow compensated optical coherence tomography of choroidal vasculature. *Sci Rep* 2018; 8: 6461.
35. Agrawal R, Seen S, Vaishnavi S, et al. Choroidal vascularity index using swept-source and spectral-domain optical coherence tomography: a comparative study. *Ophthalmic Surg Lasers Imaging Retina* 2019; 50(2): e26–e32.
36. Balestrieri E, Daponte P, Rapuano S, et al. Choroidal vessel characterization using en-face optical coherence tomography measurement. In: *2014 IEEE international symposium on medical measurements and applications (MeMeA)*, Lisboa, 11–12 June 2014, pp. 1–6. New York: IEEE.
37. Sonoda S, Sakamoto T, Yamashita T, et al. Luminal and stromal areas of choroid determined by binarization method of optical coherence tomographic images. *Am J Ophthalmol* 2015; 159: 1123.e1–1131.e1.